Chemical imaging of organic materials with MeV SIMS using a continuous collimated ion beam

Zdravko Siketić[1, *], Iva Bogdanović Radović[1], Marko Barac[1,2], Marko Brajković[1] and Marijana Popović Hadžija[1]

[1]Ruđer Bošković Institute, Bijenička c. 54, HR-10000 Zagreb, Croatia

[2]Jožef Stefan International Postgraduate School, Jamova c. 39, SLO-1000 Ljubljana, Slovenia

[*]Corresponding author: zsiketic@irb.hr

Abstract

MeV SIMS is a type of secondary ion mass spectrometry technique (SIMS) where molecules are desorbed from the sample surface with ions of MeV energies. In this work, we present a novel system for molecular imaging of organic materials using a continuous analytical beam and a start trigger for timing based on the detection of secondary electrons. The sample is imaged by the collimated primary ion beam and scanning of the target with a lateral resolution of ~ 20 μm. The mass of the analysed molecules is determined with a reflectron type time-of-flight (TOF) analyser, where the START signal for the TOF measurement is generated by the secondary electrons emitted from the thin carbon foil (~ 5 nm) placed over the beam collimator. With this new configuration of the MeV SIMS setup, a primary ion beam with the highest possible electronic stopping can be used (i.e., highest secondary molecular yield), and samples of any thickness can be analysed. Since the electrons are collected from the thin foil rather than from the sample surface, the detection efficiency of secondary electrons is always the same for any type of analysed material. Due to the ability to scan the samples by piezo stage, samples of a few cm in surface size can be imaged. The imaging capabilities of MeV SIMS are demonstrated on crossing ink lines deposited on the paper, a thin section of a mouse brain and on a fingerprint deposited on a thick Si wafer to show the potential application of the presented technique for analytical purposes in biology and forensics science.

Introduction

MeV SIMS is a recently developed ion beam analysis technique used for chemical imaging of organic materials in several laboratories worldwide [1-5]. Due to the nature of the interaction of MeV ions with the material, mainly through electronic stopping, the probability of intact molecular desorption is much higher compared to SIMS where a monoatomic primary ion beam with keV energy is used [6-9], and it correlates with the increase in electronic energy stopping power [10, 11]. Compared to the other SIMS imaging techniques, it can be placed between keV SIMS and cluster ion SIMS techniques in terms of molecular detection efficiency and achievable lateral resolution [12-13]. In general, molecules up to a mass of 1000 Da can be detected (e.g., carbohydrates and lipids), with a lateral resolution of up to 400 nm [15]. To date, we have successfully used MeV SIMS to analyse lipids in the mice liver fed with a standard or a high-fat diet [16]. At the same time, we have developed the MeV SIMS technique in the so-called "transmission" mode, which allowed us to perform two-dimensional mapping of lipids within a

single cell with a spatial resolution of 400 nm [15]. This is generally one of the few SIMS setups that can map organic samples with a spatial resolution of less than one micrometre. In addition to applications in biology, MeV SIMS has also been used to identify synthetic organic pigments in modern paint materials [17-19] and in forensics to determine the deposition order of different inks at the crossing lines [20-22]. Recently, a new MeV SIMS system for chemical-biological mapping has been developed based on collimation of the beam with a glass capillary [23, 24]. The great advantage of the MeV SIMS setup presented in [23] is the ability to accept a wide range of energies and masses of primary ions, especially high energy heavy ions that have high electronic stopping power. According to the work of M. Brajkovic et al [11], these ions should provide a largest yield of intact molecules, which is crucial for SIMS imaging. Moreover, no active elements are used for ion focusing, so the size of the beam spot should be virtually independent of the type and energy of the ions. Regardless the good results published in [23], two main problems have been identified for MeV SIMS imaging based on the collimated beam with the glass capillary:

1. Despite a good lateral resolution (between 3-20 μm) almost 50% of the beam ends in beam halo blurring 2D chemical images and raising the minimum detection limit.
2. The START signal for TOF measurement is generated by the secondary electrons emitted from the sample surface, which can be problematic for samples with low secondary electron emission (consequently low detection efficiency). Even more, variation in the secondary electron emission efficiency over the sample surface leads to the unrealistic variations in the 2D chemical images, since each image pixel is normalised to the incoming number of primary ions.

To eliminate above mentioned problems, glass capillary was replaced with an ordinary collimator used in electron microscopy with an aperture of 10 μm thus removing beam halo. Instead of detecting the secondary electrons emitted from the sample surface needed for the START signal in TOF (note that a continuous ion beam is used), secondary electrons generated by the passage of the primary ions through the thin carbon film (~ 5 nm) located above the beam collimator was used providing that START signal is independent on the type and composition of the studied sample. Moreover, the sample can be of any thickness, in contrast to the continuous primary ion beam setup presented in the work of Z. Siketic et al [15], which requires thin samples transparent for the ion beam.

In the following chapters, the new MeV SIMS setup is presented, based on collimation of the ions with a collimator and timing by secondary electrons from a thin carbon foil. In addition, the performance of the new setup is demonstrated using chemical imaging on several different samples such as ink crossing lines on the paper, thin section of a mouse brain and a fingerprint deposited on a thick Si wafer.

Experimental setup

A photograph of the interior of the MeV SIMS chamber with collimated beam is shown in Figure 1. The beam collimator, the secondary electron detector (SE), the piezo stage with the sample holder, and the extractor to the TOF reflectron spectrometer are labelled. Secondary molecules are analysed by TOF reflectron spectrometer with a 10 kV post acceleration (from © Kore Technology Ltd).

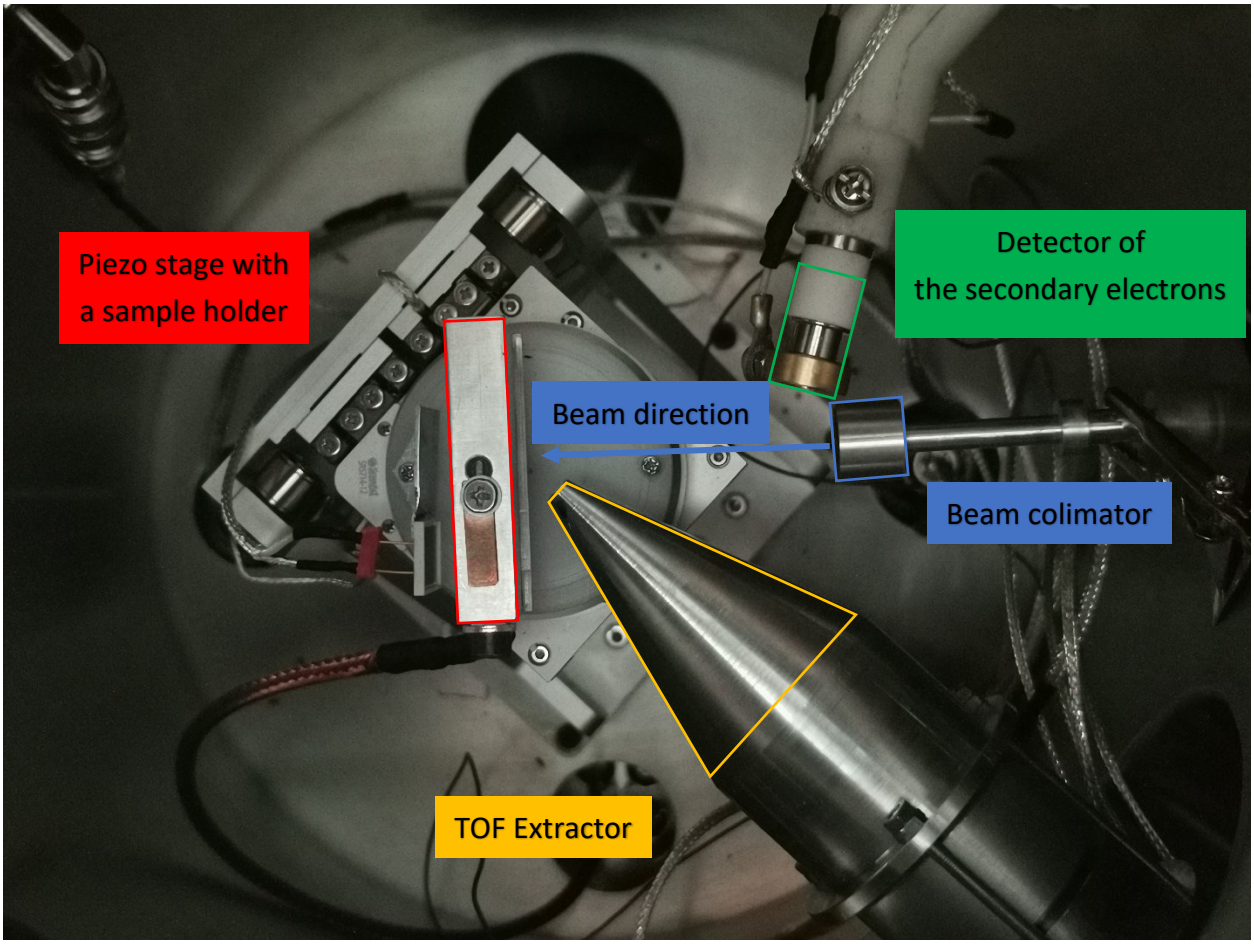

Fig. 1. Photo of the inside of the MeV SIM chamber with collimated beam.

The beam is collimated by the collimator with a central aperture of 10 µm. A ~ 5 nm carbon foil is mounted over the collimator for secondary electron generation by the primary ion beam. The desorbed molecules are accelerated towards the spectrometer by the voltage difference of + 3 kV applied to the sample holder (the TOF extractor is always grounded). The triggering system for the electron START (for TOF measurement) is similar to the system presented in reference [23]. Initially, the extraction voltage is at zero potential to ensure that the generated secondary electrons are not attracted towards the sample holder. When ion passes through the carbon foil, secondary electrons are emitted and deflected toward the SE detector, whose front electrode is at +600 V. Upon electron detection, the signal from the SE detector is used to trigger high voltage switch (HV) (Behlke HTS 61-01-GSM) to increase the extraction voltage at the target to a value of +3 kV. Since some time is required for signal processing and transport, the extraction of molecules is delayed by about 100 ns, so no significant loss of secondary ions is expected during this delay for a 3.5 mm long extraction region. HV on target is "on" for a period of 2 µs, which is sufficient to extract and collect all molecules in the mass range up to 1000 Da. During the period of TOF

measurement (~100 µs), there is a VETO for the data acquisition system (DAQ) to accept another START signal and start a new increase in extraction voltage through the HV switch. In this way, the probability of random coincidences is minimised and the random noise in the mass spectra is reduced.

The measured ion detection efficiency by secondary electrons is around 20%. This was estimated from the time required to produce the same statistics in the mass spectra in the "transmission" mode (100% ion detection efficiency). Thus, for the same number of secondary ions, about 5 more primary ions are required. It must be emphasised that in addition to the secondary electrons emitted from the carbon foil, electrons produced by ion scattering from the collimator edge are also detected, producing the "false" START signals. Since the ions scattered from the collimator edge usually do not reach the target, there are no secondary molecules desorbed by them, so these events do not contribute to the noise in the mass spectra. As mentioned in the introduction, the samples are mounted on the sample holder connected to the xyzθ piezo stage, with travel range of ±31.5 mm in the x, y, and z directions and an integrated sensor with ~1 nm resolution. This allows precise lateral imaging of samples up to several cm in size, subject to primary ion current, available measurement time and statistics required. The rotation axis is used to optimise the extraction angle to the TOF extractor. The movement/scanning of the piezo stage is controlled by the in-house built DAQ system Spector [25] and synchronised with the TOF spectrometer. The sample is scanned in pixel-by-pixel mode (the number of pixels and step size are set in the DAQ system by the user), with each pixel normalised to the same number of incoming particles based on the number of counts from the SE detector. It takes about three hours to produce an image consisting of 100 x 100 pixels with reasonable spectral statistics in each pixel. The main limitation on DAQ imaging time is the low current of the primary ion beam, which is few fA after the collimator.

Results

1. Beam lateral resolution measurement

The beam profile and lateral resolution test of the 14 MeV Cu^{4+} ion beam was performed on a Gafchromic EBT3 film sensitive to the ion beam radiation and on a patterned phthalocyanine grid ($C_{32}H_{18}N_8$) deposited on a Si wafer (440 µm step). The purpose of these measurements was to study the ion beam halo and to show the influence of the ~ 5 nm carbon foil on the lateral ion beam straggling and the resolution by the 10 µm aperture collimator.

As can be seen in Fig. 2, there is virtually no beam halo after collimation (up to the film sensitivity), which is a significant improvement comparing to the beam profile after collimation through the glass capillary [23]. Only the central ion beam spot is visible.

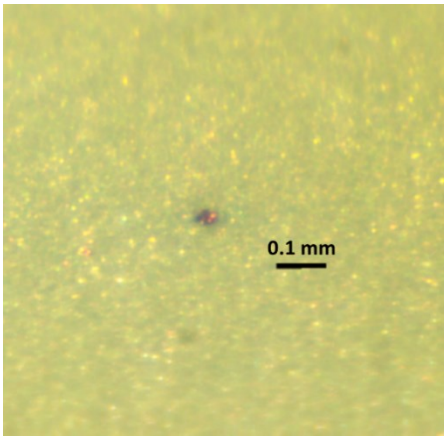

Figure 2. Image of the collimated 14 MeV Cu^{4+} ion beam on Gafchromic EBT3 film (10 µm aperture)

MeV SIMS image of the patterned phthalocyanine vapour deposited onto the Si wafer through the 440 µm grid is shown in Fig. 3. The different intensities in the phthalocyanine region are caused by the non-uniform lateral distribution during the evaporation process.

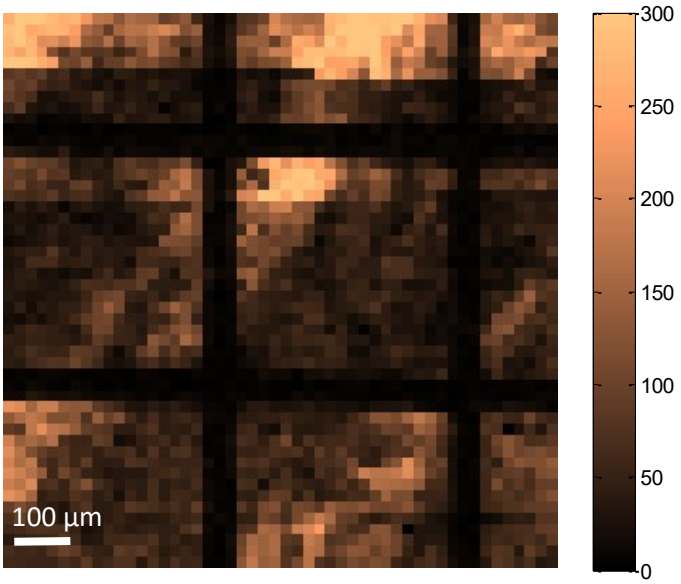

Figure 3. MeV SIMS image of patterned phthalocyanine grid with 440 µm step. Image size is 1mm x 0.9 mm.

According to the results in Fig. 3, the lateral resolution of the ion beam is less than one pixel, i.e., less than pixel size which is 20 µm. Assuming a collimator aperture of 10 µm, the lateral ion beam straggling through the 5 nm carbon foil contributes less than $\sqrt{20^2 - 10^2}\mu m \approx 17\ \mu m$ to the total lateral resolution. For

example, there is no significant difference in lateral resolution between a 5 µm and a 10 µm collimator, but the ion beam current is higher by a factor of 4 in the latter case.

2. MeV SIMS imaging by continuous collimated ion beam

The imaging capabilities of the presented MeV SIMS system are demonstrated on an ink crossing line deposited on a paper, a thin section of a mouse brain, and a fingerprint deposited on a Si wafer. The 14 MeV Cu^{4+} ion beam was used for all presented MeV SIMS measurements.

a. MeV SIMS imaging of the ink crossing lines

Fig. 4 shows the MeV SIMS image of the crossing lines of ink deposited on the paper: a) 2D map of BV3 pigment molecular peaks (358-372 Da) and b) the corresponding mass spectra.

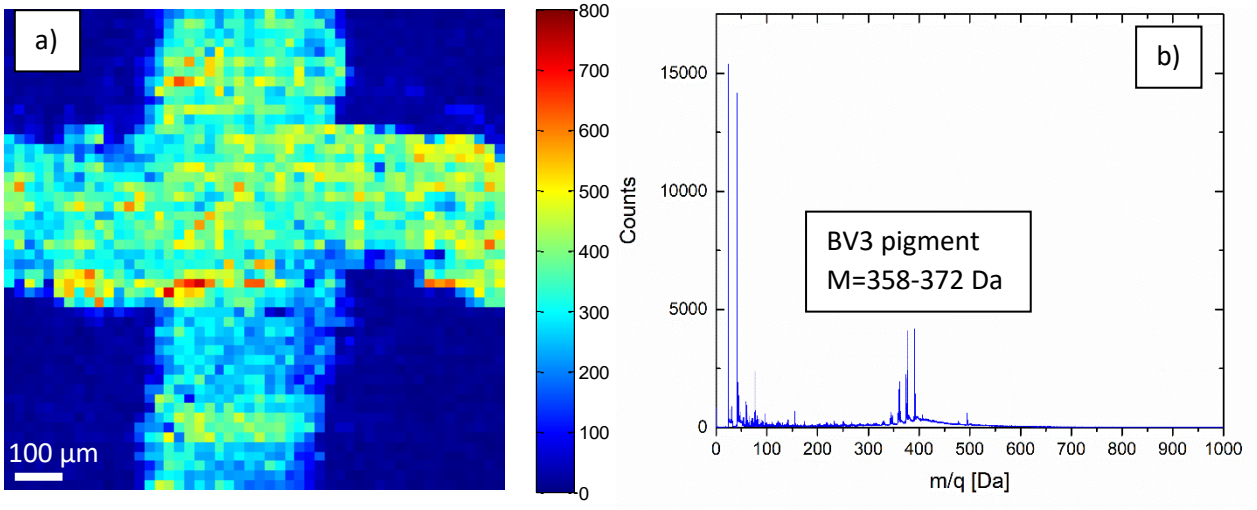

Figure 4. a) MeV SIMS image of ink crossing lines (map of the selected BV3 pigment, M=358-372 Da). b) Corresponding MeV SIMS mass spectra. Image size is 1mm x 1mm.

The same sample was imaged by ions collimated though the glass capillary (results are presented in ref. [23]). Comparing these two measurements, it is immediately apparent that the image produced with the ion beam collimated by a simple aperture is clearer with a better contrast (~ 20 times higher signal-to-noise ratio in the image). High image quality is provided due to the significantly lower beam halo compared to the beam collimation by glass capillary.

b. MeV SIMS imaging of mouse brain thin section

Mouse brain thin section was prepared according to standard protocols for SIMS analysis [26]. To preserve brain morphology and primary distribution of molecular species, a portion of the tissue was immediately embedded in Tissue-Tek OCT Compound for Cryostat Sectioning (Sakura, The Netherlands), cryopreserved in isopentane cooled with liquid nitrogen, and stored at -80°C until cryo-sectioning. OCT-embedded blocks of frozen brain tissue were removed from the freezer and sectioned inside a cryostat microtome held at -25°C. Thin sections of mouse brain were mounted on a Si wafer and placed in the vacuum chamber for MeV SIMS analysis (the base vacuum was ~10^{-7} mbar). Obtained MeV SIMS images of selected mass peaks (lipid fragment M=184.1 Da, cholesterol M=369.4 Da and OCT medium M=228.4 Da) and mass spectra are shown in Fig. 5. The corresponding optical image is also displayed (image size: 2 mm x 2 mm).

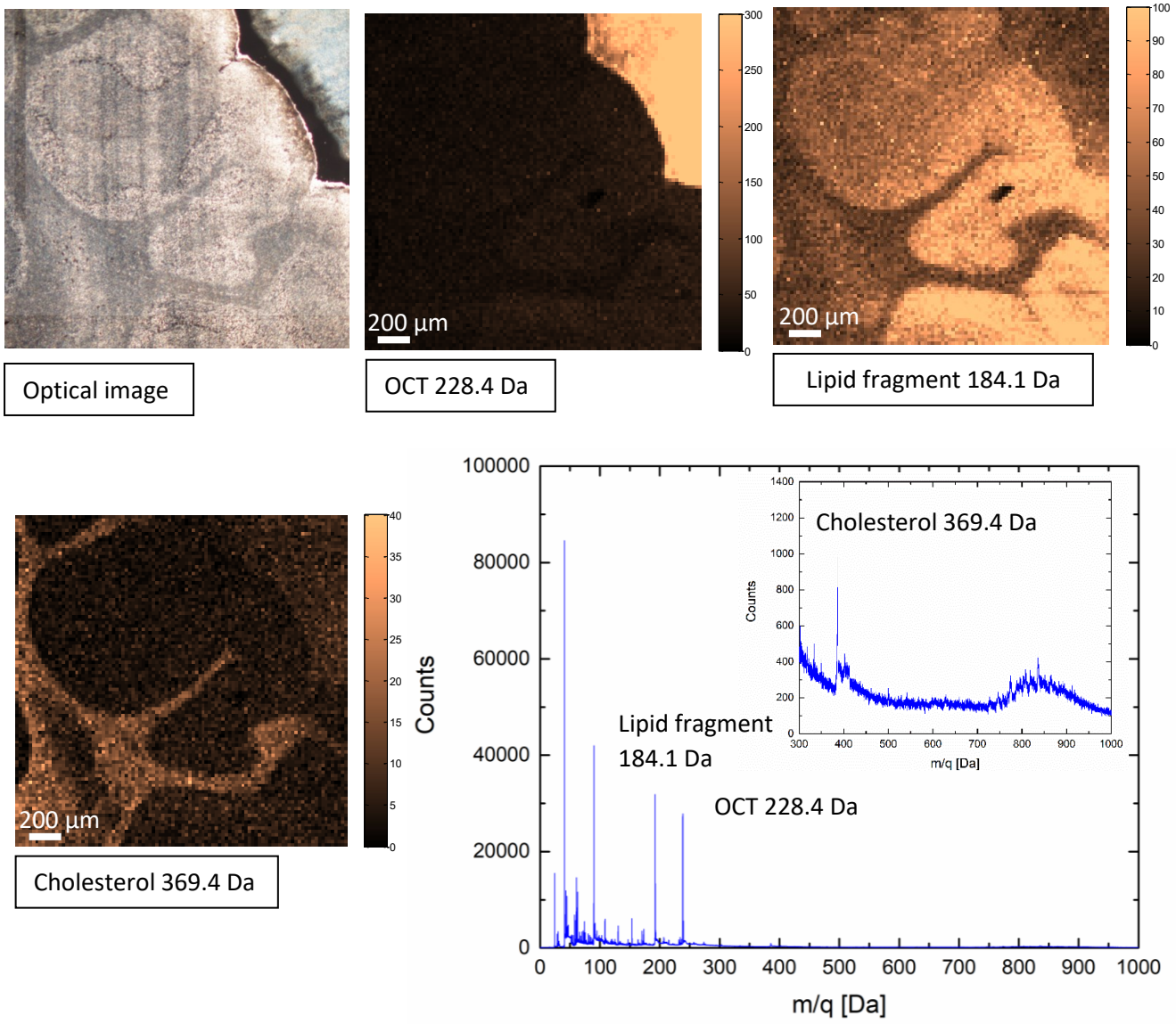

Figure 5. MeV SIMS and optical images of thin section of mouse brain (image size: 2 mm x 2 mm). Molecular maps of OCT medium (M=228.4 Da), lipid fragment (M=184.1 Da), and cholesterol (M=369.4 Da) are shown. Corresponding mass spectra with inset shoving cholesterol peak are presented as well.

Comparison of MeV SIMS and optical images shows that lipids, as the main composition of myelin's sheath around nerve fibre, are mostly located in the white matter. Contrary, cholesterol is mostly placed in the brain's grey matter. The grey matter is built form the bodies of nerve cells whose membranes contain cholesterol. In addition, OCT medium is located only outside the tissue region, indicating that sample is not contaminated with medium during preparation.

c. MeV SIMS imaging of the fingerprint

A fresh fingerprint was deposited on a clean Si wafer and placed in the vacuum chamber. The MeV SIMS image (total number of ions) and corresponding optical image are shown in Fig. 6. The image size is 5 mm x 5 mm.

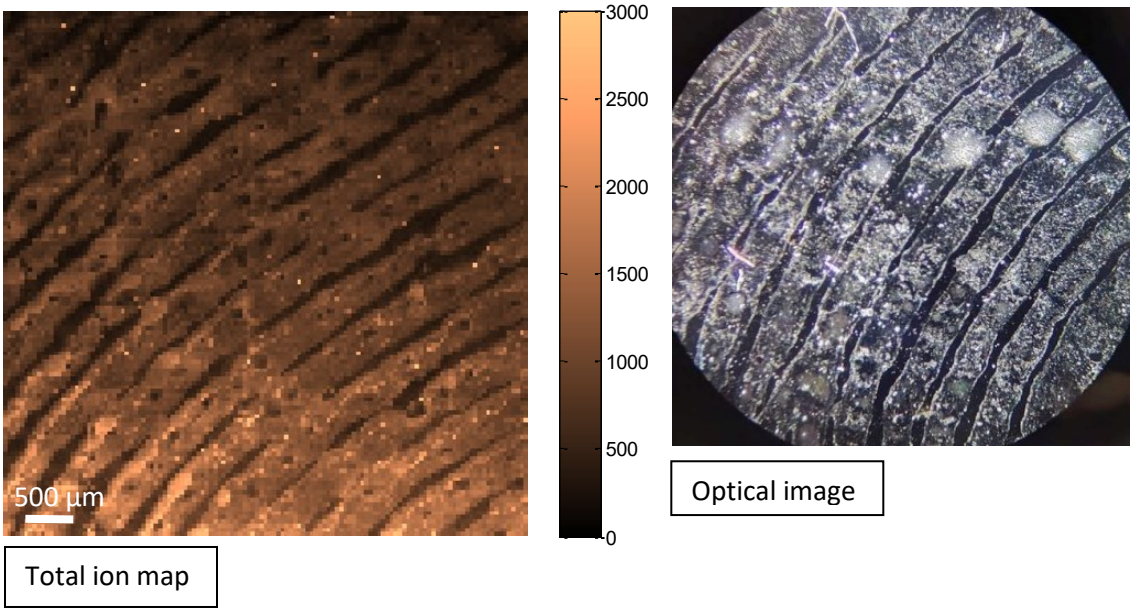

Figure 6. Total ion map of the fingerprint analysed by MeV SIMS (image size: 5 mmx 5 mm). Corresponding optical image is shown as well.

As can be seen, the friction ridges of the fingerprint as well as the sweat pores are clearly resolved and visible. Only a portion of the fingerprint is measured, but due to the ~30 mm travel of the piezo stage, the entire fingerprint can be imaged in a single run. In addition to the image, the molecular composition of the fingerprint can also be determined, which may be of particular interest for forensic investigations. In particular case, among other molecular peaks, cholesterol and diacylglycerols are identified in the fingerprint.

Conclusions

In this work, we have demonstrated imaging abilities of a new MeV SIMS setup based on the continuous collimated ion beam (simple 10 μm aperture is used for collimation) with a target-independent system for START trigger in TOF measurements by using secondary electrons emitted from the 5 nm carbon foil placed over the beam collimator. By replacing the glass capillary with a simple collimator, the ion beam halo becomes negligible, dramatically improving imaging capabilities. This is particularly evident by comparing MeV SIMS images of ink crossing lines made with the old system based on the glass capillary collimation, and the system presented here. The imaging capabilities of the new system were tested on three different types of samples. From the results it is clear that system has great potential for chemical imaging of biological and forensic samples, especially larger ones (up to a few cm) with a modest lateral resolution (less than 20 μm).

Acknowledgments

M. Brajković acknowledges support by the Croatian Science Foundation (CSF) project "Young Researchers' Career Development Project - Training of Doctoral Students" co-financed by the European Union, Operational Program "Efficient Human Resources 2014-2020" and the ESF. I. B. R. and Z. S. acknowledge support by the CSF project IP-2016-06-1698 "Development of a capillary microprobe for MeV SIMS for analysis of biological materials– BioCapSIMS" and by the RADIATE project under the Grant Agreement 824096 from the EU Research and Innovation program HORIZON 2020. The authors also acknowledge financial support from the European Regional Development Fund for the 'Center of Excellence for Advanced Materials and Sensing Devices' (Grant No. KK.01.1.1.01.0001).

References

[1] Y. Nakata, Y. Honda, S. Ninomiya, T. Seki, T. Aoki, and J. Matsuo, "*Matrixfree high-resolution imaging mass spectrometry with high-energy ion projectiles*," J. Mass Spectrom., vol. 44, no. 1, pp. 128–136, 2009.

[2] T. Tadic, I. B. Radovic, Z. Siketic, et al., "*Development of a TOF SIMS setup at the Zagreb heavy ion microbeam facility*," Nucl. Instr. and Meth. B, vol. 332, pp. 234–237, 2014.

[3] B. N. Jones, V. Palitsin, and R. Webb, "*Surface analysis with high energy time of-flight secondary ion mass spectrometry measured in parallel with PIXE and RBS*," Nucl. Instr. and Meth. B, vol. 268, no. 11-12, pp. 1714–1717, 2010.

[4] L. Jeromel, Z. Siketic, N. O. Potocnik, et al.,"*Development of mass spectrometry by high energy focused heavy ion beam: MeV SIMS with 8 MeV Cl7+ beam*," Nucl. Instr. and Meth. B, vol. 332, pp. 22–27, 2014.

[5] M. Schulte-Borchers, M. Doebeli, A. M. Muller, M. George, and H.-A. Synal, "*Time of-flight MeV-SIMS with beam induced secondary electron trigger*," Nul. Instr. and Meth., vol. 380, pp. 94–98, 2016.

[6] R. D. Macfarlane and D. F. Torgerson, "*Californium-252 Plasma Desorption Mass Spectroscopy*", Science, vol. 191, no. 4230, pp. 920–925, 1976.

[7] E. D. Silveira, C. McAfee, D. Cocke, D. Naugle, D. Sun, and E. Schweikert, "*Particle desorption mass spectrometry of YBCO superconductors*", Int. J. Mass Spectrom. Ion Processes, vol. 91, no. 2, R5–R11, 1989.

[8] H. Feld, R. Zurmuehlen, A. Leute, and A. Benninghoven, *"Carbon cluster emission from polymers under keV and MeV ion bombardment*," J. Phys. Chem., vol. 94, no. 11, pp. 4595–4599, 1990.

[9] B. N. Jones, J. Matsuo, Y. Nakata, et al., "*Comparison of MeV monomer ion and keV cluster ToF-SIMS*," Surf. Interface Anal., vol. 43, no. 1-2, pp. 249–252, 2010.

[10] M. Toulemonde, E. Paumier, and C. Dufour, "*Thermal spike model in the electronic stopping power regime*", Radiat. Eff. Defects Solids, vol. 126, no. 1-4, pp. 201–206, 1993.

[11] M. Brajkovic, M. Barac, I. Bogdanovic Radovic, and Z. Siketic, "*Dependence of Megaelectron Volt time-of-flight secondary ion mass spectrometry secondary molecular ion yield from phthalocyanine blue on primary ion stopping power*", J. Am. Soc. Mass. Spectrom., vol. 31, no. 7, pp. 1518–1524, 2020.

[12] J. S. Fletcher, N. P. Lockyer, and J. C. Vickerman, "*Molecular SIMS imaging; spatial resolution and molecular sensitivity: have we reached the end of the road? Is there light at the end of the tunnel?*" Surf. Interface Anal. 43, 253, 2011

[13] N. Winograd, "*Gas Cluster Ion Beams for Secondary Ion Mass Spectrometry*", Annu. Rev. Anal. Chem. 11:29–48, 2018

[14] Hua Tian, Sadia Sheraz née Rabbani, John C. Vickerman, and Nicholas Winograd, "*Multiomics Imaging Using High-Energy Water Gas Cluster Ion Beam Secondary Ion Mass Spectrometry [$(H2O)_n$-GCIB-SIMS] of Frozen-Hydrated Cells and Tissue*" Anal. Chem., 93, 22, 7808–7814, 2021

[15] Z. Siketic, I. B. Radovic, M. Jaksic, M. P. Hadzija, and M. Hadzija, "*Submicron mass spectrometry imaging of single cells by combined use of mega electron volt time-of-flight secondary ion mass spectrometry and scanning transmission ion microscopy*," Appl. Phys. Lett., vol. 107, no. 9, p. 093 702, 2015.

[16] M. Popović Hadžija, Z. Siketić, M. Hadžija, M. Barac, I. Bogdanović Radović, "*Study of the diacylglycerol composition in the liver and serum of mice with prediabetes and diabetes using MeV TOF-SIMS"*, Diabetes research and clinical practice, 159, 107986, 9, 2020

[17] M. Krmpotić, D. Jembrih Simburger, Z. Siketić, M. Anghelone, I. B. Radović*, "Study of UV ageing effects in modern artists' paints with MeV-SIMS"*, Polymer Degradation and Stability 195, 109769, 2022

[18] M. Krmpotić, D. Jembrih-Simbürger, Z. Siketić, N. Marković, M. Anghelone, T. Tadić, D. Plavčić, M. Malloy, I. Bogdanović Radović, "*Identification of Synthetic Organic Pigments (SOPs) Used in Modern Artist's Paints with Secondary Ion Mass Spectrometry with MeV Ions"*, Anal. Chem., 92, 13, 9287–9294, 2020

[19] 17. I. Bogdanović Radović, Z. Siketić, D. Jembrih-Simbürger, N. Marković, M. Anghelone, V. Stoytschew, M. Jakšić, "*Identification and imaging of modern paints using Secondary Ion Mass Spectrometry with MeV ions"*, Nucl. Instr. and Meth. B 406, 296, 2017

[20] M. Malloy, I. Bogdanović Radović, Z. Siketić, M. Jakšić, "*Determination of deposition order of blue ballpoint pen lines by MeV SIMS"*, Forensic Chemistry 7, 75, 2018

[21] Moore, K. L.; Barac, M.; Brajkovic, M.; Bailey, M. J.; Siketic, Z.; Bogdanovic Radovic, I., *"Determination of deposition order of toners, inkjet inks, and blue ballpoint pen combining MeV-secondary ion mass spectrometry and particle induced X-ray emission"* Anal. Chem., 91 (20), 12997-13005, 2019

[22] M. Barac, A. Filko, M. Brajković, Z. Siketić, A. Ledić, I. B. Radović, "*Comparison of optical techniques and MeV SIMS in determining deposition order between optically distinguishable and indistinguishable inks from different writing tools"*, Forensic Science International 331, 111136, 2022

[23] M. Brajković, I. Bogdanović Radović, M. Barac, D. D. Cosic, Z. Siketić, "*Imaging of Organic Samples with Megaelectron Volt Time-of-Flight Secondary Ion Mass Spectrometry Capillary Microprobe"*, J. Am. Soc. Mass Spectrom., 32, 10, 2567–2572, 2021

[24] M. Brajković, M. Barac, D. Cosic, I. Bogdanović Radović, Z. Siketić, "*Development of MeV TOF-SIMS capillary microprobe at the Ruđer Bošković Institute in Zagreb"*, Nucl. Instr. and Meth. B 461, 237-242, 2019

[25] D. Cosic, M. Bogovac, M. Jakšić, "*Data acquisition and control system for an evolving nuclear microprobe*", Nucl. Instr. and Meth. B 451, 122–126, 2019.

[26] J. Malm, D. Giannaras, M. O. Riehle, N. Gadegaard, and P. Sjovall, *Fixation and Drying Protocols for the Preparation of Cell Samples for Time-of-Flight Secondary Ion Mass Spectrometry Analysis*, Anal. Chem. 81 (2009), 7197-7205.